Development and underground test of radiopure ZnMoO4 scintillating bolometers for the LUMINEU 0 nu 2 beta project

E. Armengaud, Q. Arnaud, C. Augier, A. Benoit, L. Berge, S. Boiko R., T. Bergmann, J. Blueme, A. Broniatowski, V. Brudanin, et al.

Development and underground test of radiopure ZnMoO$_4$ scintillating bolometers for the LUMINEU $0v2\beta$ project

E. Armengaud[a], **Q. Arnaud**[b], **C. Augier**[b], **A. Benoît**[b], **A. Benoît**[c], **L. Bergé**[d],
R.S. Boiko[e], **T. Bergmann**[f], **J. Blümer**[g,h], **A. Broniatowski**[d], **V. Brudanin**[i], **P. Camus**[c],
A. Cazes[b], **M. Chapellier**[d], **F. Charlieux**[b], **D.M. Chernyak**[d,e], **N. Coron**[j], **P. Coulter**[k],
F.A. Danevich[e], **T. de Boissière**[a], **R. Decourt**[l], **M. De Jesus**[b], **L. Devoyon**[m],
A.-A. Drillien[d], **L. Dumoulin**[d], **K. Eitel**[h], **C. Enss**[n], **D. Filosofov**[i], **A. Fleischmann**[n],
N. Foerster[g], **N. Fourches**[a], **J. Gascon**[b], **L. Gastaldo**[n], **G. Gerbier**[a], **A. Giuliani**[d,o,p*],
D. Gray[a], **M. Gros**[a], **L. Hehn**[h], **S. Henry**[k], **S. Hervé**[a], **G. Heuermann**[g], **V. Humbert**[d],
I.M. Ivanov[q], **A. Juillard**[b], **C. Kéfélian**[b,g], **M. Kleifges**[f], **H. Kluck**[g,†], **V.V. Kobychev**[e],
F. Koskas[m], **V. Kozlov**[h], **H. Kraus**[k], **V.A. Kudryavtsev**[r], **H. Le Sueur**[d], **M. Loidl**[s],
P. Magnier[a], **E.P. Makarov**[q], **M. Mancuso**[d,t], **P. de Marcillac**[d], **S. Marnieros**[d],
C. Marrache-Kikuchi[d], **A. Menshikov**[f], **S.G. Nasonov**[q], **X.-F. Navick**[a], **C. Nones**[a],
E. Olivieri[d], **P. Pari**[u], **B. Paul**[a], **Y. Penichot**[a], **G. Pessina**[p,v], **M.C. Piro**[d], **O. Plantevin**[d],
D.V. Poda[d,e], **T. Redon**[j], **M. Robinson**[r], **M. Rodrigues**[s], **S. Rozov**[i], **V. Sanglard**[b],
B. Schmidt[h], **S. Scorza**[g], **V.N. Shlegel**[q], **B. Siebenborn**[h], **O. Strazzer**[m],
D. Tcherniakhovski[f], **M. Tenconi**[d], **L. Torres**[j], **V.I. Tretyak**[e,w], **L. Vagneron**[b],
Ya.V. Vasiliev[q], **M. Velazquez**[l], **O. Viraphong**[l], **R.J. Walker**[h], **M. Weber**[f], **E. Yakushev**[i],
X. Zhang[k], **and V.N. Zhdankov**[x] (the LUMINEU and the EDELWEISS collaborations)

^{a}CEA, Centre d'Etudes Saclay, IRFU, 91191 Gif-Sur-Yvette Cedex, France

^{b}IPNL, Université de Lyon, Université Lyon 1, CNRS/IN2P3, 69622 Villeurbanne cedex, France

^{c}CNRS-Néel, 38042 Grenoble Cedex 9, France

^{d}CSNSM, Centre de Sciences Nucléaires et de Sciences de la Matière, CNRS/IN2P3, Université Paris-Sud, 91405 Orsay, France

^{e}Institute for Nuclear Research, MSP 03680 Kyiv, Ukraine

^{f}Karlsruhe Institute of Technology, Institut für Prozessdatenverarbeitung und Elektronik, 76021 Karlsruhe, Germany

^{g}Karlsruhe Institute of Technology, Institut für Experimentelle Kernphysik, 76128 Karlsruhe, Germany

^{h}Karlsruhe Institute of Technology, Institut für Kernphysik, 76021 Karlsruhe, Germany

^{i}Laboratory of Nuclear Problems, JINR, 141980 Dubna, Moscow region, Russia

^{j}IAS, CNRS, Université Paris-Sud, 91405 Orsay, France

^{k}University of Oxford, Department of Physics, Oxford OX1 3RH, UK

^{l}ICMCB, CNRS, Université de Bordeaux, 33608 Pessac Cedex, France

^{m}CEA, Centre d'Etudes Saclay, Orphée, 91191 Gif-Sur-Yvette Cedex, France

^{n}Kirchhoff Institute for Physics, Heidelberg University, D-69120 Heidelberg, Germany

^{o}Dipartimento di Scienza e Alta Tecnologia dell'Universit'a dell'Insubria, 22100 Como, Italy

^{p}INFN, Sezione di Milano-Bicocca, 20126 Milano, Italy

^{q}Nikolaev Institute of Inorganic Chemistry, 630090 Novosibirsk, Russia

^{r}Department of Physics and Astronomy, University of Sheffield, Hounsfield Road, Sheffield S3 7RH, UK

^{s}CEA, LIST, LNHB, 91191 Gif-Sur-Yvette Cedex, France

^{t}Dipartimento di Scienza e Alta Tecnologia dell'Universitá dell'Insubria, I-22100 Como, Italy

^{u}CEA, Centre d'Etudes Saclay, IRAMIS, 91191 Gif-Sur-Yvette Cedex, France

^{v}Dipartimento di Fisica dell'Universitá di Milano-Bicocca, 20126 Milano, Italy

^{w}INFN, Sezione di Roma "La Sapienza", 00185 Rome, Italy

^{x}CML Ltd., 630090 Novosibirsk, Russia

†present address: Institut für Hochenergiephysik der Österreichischen Akademie der Wissenschaften, A-1050 Wien, Austria

E-mail: Andrea.Giuliani@csnsm.in2p3.fr

ABSTRACT: The LUMINEU (Luminescent Underground Molybdenum Investigation for NEUtrino mass and nature) project envisages a high-sensitivity search for neutrinoless double beta ($0\nu2\beta$) decay of ^{100}Mo with the help of scintillating bolometers based on zinc molybdate (ZnMoO$_4$) crystals. One of the crucial points for the successful performance of this experiment is the development of a protocol for producing high quality large mass ZnMoO$_4$ crystal scintillators with extremely high internal radiopurity. Here we report a significant progress in the development of large volume ZnMoO$_4$ crystalline boules (with mass up to 1 kg) from deeply purified materials. We present and discuss the results achieved with two ZnMoO$_4$ samples (with mass of about 0.3 kg each): one is a precursor of the LUMINEU project, while the other one was produced in the framework of LUMINEU with an improved purification / crystallization procedure. The two crystals were measured deep underground as scintillating bolometers in the EDELWEISS dilution refrigerator at the Laboratoire Souterrain de Modane (France) protected by a rock overburden corresponding to 4800 m w.e. The results indicate that both tested crystals are highly radiopure. However, the advanced LUMINEU sample shows a clear improvement with respect to the precursor, exhibiting only a trace internal contamination related with ^{210}Po at the level of 1 mBq/kg, while the activity of ^{226}Ra and ^{228}Th is below 0.005 mBq/kg. This demonstrates that the LUMINEU purification and crystal-growth procedures are very efficient and leads to radiopurity levels which exceedingly satisfy not only the LUMINEU goals but also the requirements of a next-generation $0\nu2\beta$ experiment.

KEYWORDS: Double-beta decay detectors; Cryogenic detectors; Scintillators, scintillation and light emission processes (solid, gas and liquid scintillators); Hybrid detectors.

---

*Corresponding author.

Contents

1. Introduction

The LUMINEU (Luminescent Underground Molybdenum Investigation for NEUtrino mass and nature) project [1] aims to develop a technology based on scintillating bolometers – heat-light double read-out cryogenic detectors – to be applied to high-sensitivity searches for neutrinoless double beta ($0\nu2\beta$) decay [2], as it was discussed in Ref. [3] and more recently in Ref. [4]. The interest in this hypothetical very rare process, in which two neutrons inside a nucleus transform simultaneously into two protons with the emission of two electrons and nothing else, is related to several underlying fundamental problems. In general, the observation of the $0\nu2\beta$ decay would indicate lepton number non-conservation and therefore the existence of physics beyond the Standard Model of elementary particles (see e.g. Ref. [5]). The $0\nu2\beta$ process can give answers to a number of fundamental questions on neutrino properties, like the Majorana nature of neutrino (i.e. its equivalence to its antiparticle), the absolute scale of the neutrino mass and the corresponding ordering of the mass eigenstates (inverted or normal hierarchy), the values of the Majorana CP-violating phases and other effects (more details can be found in the recent reviews [5, 6, 7] and references therein).

   The LUMINEU collaboration intends to perform a pilot experiment to search for $0\nu2\beta$ decay of ^{100}Mo by using scintillating bolometers based on zinc molybdate (ZnMoO$_4$) crystal scintillators containing $\sim$1 kg of enriched ^{100}Mo [1, 8]. The successful accomplishment of the LUMINEU program would set the foundations for a next-generation $0\nu2\beta$ decay bolometric experiment capable to explore the inverted hierarchy region of the neutrino mass pattern [3, 4]. One of the most challenging tasks of LUMINEU is the development of a protocol for the production of large mass ($\sim$1 kg) ZnMoO$_4$ crystals with excellent optical quality and high radiopurity, as well as the reproducibility of the crystal growth. The difficulty of this task can be appreciated by considering the quite low quality and the modest size of the ZnMoO$_4$ samples available at the beginning of

the LUMINEU program. Although half a century had elapsed since the growth and the study of the first small $ZnMoO_4$ crystals [9, 10], no sufficient progress was reached until the last $\sim$5 years, essentially because of the weak interest in this material. A decade ago $ZnMoO_4$ scintillator was suggested as suitable candidate for the implementation of cryogenic experiments to search for rare events (dark matter and $0\nu2\beta$ decay of ^{100}Mo) in Ref. [11]. At that time, several groups were motivated to develop a technological process to grow middle volume $ZnMoO_4$ crystals. Consequently, $\sim 10 - 30$ cm^3 samples were produced in the next few years by using Kyropoulos [12] and Czochralski [12, 13] methods. Moreover, one of the samples described in Ref. [13] was tested for the first time as a scintillating bolometer [14] and demonstrated encouraging prospects for double beta decay experiments. Further progress was reached by using the Czochralski technique, which enabled the growth of reasonably large $ZnMoO_4$ crystals (up to $\oslash$44$\times$100 mm) [15]. All these samples had poor optical quality revealed by an intense yellow/orange coloration, and their size and radiopurity were not enough to plan a large-scale $0\nu2\beta$ experiment. Therefore, a new technology was required to resolve these issues in view of an application to high-sensitivity $0\nu2\beta$ searches.

This paper reports the progress on the development of large mass ($\sim$1 kg) radiopure $ZnMoO_4$ crystal scintillators in the framework of the LUMINEU project. In particular, Section 2 presents the first successful attempts to develop large $ZnMoO_4$ crystals (precursors of LUMINEU) by using the low-thermal-gradient Czochralski (LTG Cz) technique [16, 17], innovative with respect to the ones adopted in Ref. [12, 13]. This Section discusses the technological issues related to the performed R&D activities, aiming at establishing methods for deep purification of molybdenum and growth of high-quality large-volume $ZnMoO_4$ crystals. Section 3 is devoted to low-background measurements with large mass non-enriched $ZnMoO_4$ scintillating bolometers in the EDELWEISS set-up[1] at the Laboratoire Souterrain de Modane (LSM, France), which demonstrate an unprecedented radiopurity of the tested crystals.

2. Development of $ZnMoO_4$ crystal scintillators

2.1 Precursors of the LUMINEU program

Here we describe briefly the results of the initial R&D on the production of large mass $ZnMoO_4$ samples which were developed in the Nikolaev Institute of Inorganic Chemistry (NIIC, Novosibirsk, Russia) as precursors of the LUMINEU program with the help of the LTG Cz technique [16, 17]. The choice of this method is motivated by its several advantages in comparison to conventional Czochralski (Cz) technique, in particular (i) up to 90% crystal yield from initial compound (around 30% for Cz), (ii) less than 1% of powder loss (around 3% for Cz), (iii) higher optical quality of the output material thanks to lower temperature gradient and therefore (iv) better stoichiometry during crystal growth. These features are quite important for the development of high quality crystals with minimal losses from compounds with both natural and enriched isotopic composition. The LTG Cz method allows growing large size crystal scintillators, as it was demonstrated for BGO [19], $CdWO_4$ and $ZnWO_4$ [20]. This technique was applied as well to develop

---

[1]EDELWEISS (Expérience pour DEtecter Les Wimps En Site Souterrain) [18] is a dark-matter experiment based on cryogenic detectors, measuring both the phonon and ionization signals produced by particle interactions in germanium crystals. This technique allows nuclear recoil events to be distinguished from electron recoil events.

excellent optical quality and radiopurity CdWO$_4$ scintillators from cadmium enriched in ^{106}Cd [21] and ^{116}Cd [22].

All the aforementioned assets of the LTG Cz technology gave us a strong impetus towards the successful development of large mass ZnMoO$_4$ crystals. For this purpose, we used 99.995% purity grade zinc oxide (ZnO) powder provided by the Umicore company [23] and similar purity molybdenum oxide powder (MoO$_3$, 99.999%) additionally purified at NIIC. High purity of ZnO (Umicore) in terms of radioactive contamination had already been checked in low background measurements with zinc tungstate crystal scintillator produced by NIIC [24]. A high purity ZnMoO$_4$ compound was obtained by solid-phase synthesis. A first 0.9 kg ZnMoO$_4$ crystal boule with a length of about 14 cm was grown in a $\oslash$ 80 mm platinum crucible by using the LTG Cz technique [25]. The boule was grown in the [001] direction at a rotation speed of 20 rotations per minute (rpm) during the pulling process. The temperature gradient was kept below 1°C/cm. As one can see from Fig. 1 (a), the pulled large ZnMoO$_4$ crystal was slightly yellow colored. The coloration is most likely due to internal trace contamination by transition metals. The ZnMoO$_4$ samples, shown in Fig. 1 (c), were cut with an irregular shape in order to have as massive as possible detector prototypes. One 329 g ZnMoO$_4$ sample was used for low temperature tests at the Laboratori Nazionali del Gran Sasso (LNGS, Assergi, Italy) [26], while another one with mass of 313 g was used in the present study.

It is evident that a dedicated growth technology is needed to develop radiopure colorless large volume ZnMoO$_4$ crystal scintillators. This part of the LUMINEU program will be described in the next subsection.

2.2 Development of advanced quality ZnMoO$_4$ crystals

An intensive R&D activity – performed before [27] and within the LUMINEU program [28] – was devoted to systematic studies of the purification of the initial compound and to the optimization of the growing conditions. We remind here some important steps.

Significant improvement in growing colorless large ZnMoO$_4$ crystals was obtained with molybdenum deeply purified by using different techniques. In the beginning the purification was achieved by recrystallization from aqueous solutions by co-precipitation of impurities on zinc molybdate sediment. In this method, MoO$_3$ dissolved in ammonium hydroxide (NH$_4$OH) was purified by co-precipitation on zinc hydroxide (Zn(OH)$_2$) [27]. This precipitant was created by dissolving zinc oxide in ammonium molybdate with subsequent adding of ammonium hydroxide to the solution. This procedure leads to an increase of the pH level from 6–7 up to 8–9 and therefore to the creation of insoluble compounds of Fe and Zn and to the absorption of impurities by Zn(OH)$_2$. The selected solution was further purified by adding some amount of ammonium oxalate ((NH$_4$)$_2$C$_2$O$_4$), which can bind to impurity ions. Ammonium molybdate crystals were released from the solution by evaporation, and MoO$_3$ was obtained by annealing. The described purification procedure gives the possibility to grow high optical quality ZnMoO$_4$ crystals with volume up to 50 cm^3 (mass up to 200 g) by using the LTG Cz method [27]. The transmittance measurements reported in Ref. [27] clearly demonstrate the impact of purity on the coloration of ZnMoO$_4$ scintillators. The new crystals were also tested at millikelvin temperatures with satisfactory results and encouraging radiopurity [3, 27, 29, 30].

The procedure desrcibed above was improved thanks to a two-stage complex technique developed recently in the framework of the LUMINEU program [28]. A combination of double sub-
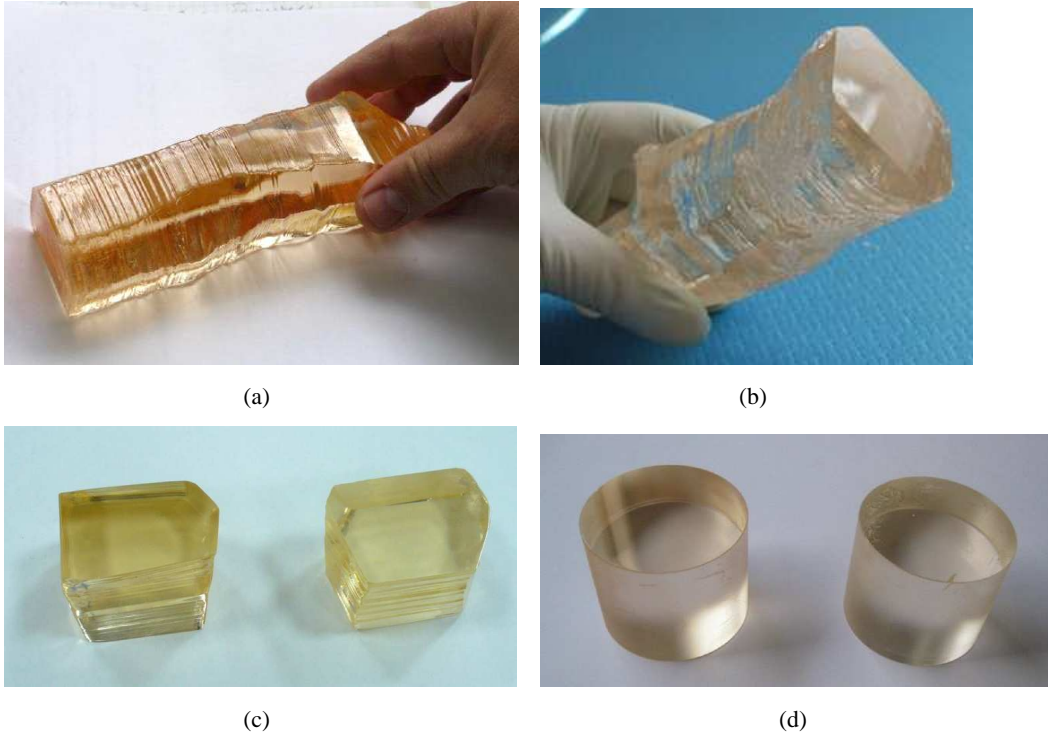
(a)   (b)

(c)   (d)

Figure 1. Large volume zinc molybdate crystal boules with mass ~ 1 kg developed as a precursor (a) and in the framework of the LUMINEU program (b) (see text). Scintillation elements with mass of about 0.3 kg produced from precursor (c) and LUMINEU (d) $ZnMoO_4$ crystal boules.

limation (with addition of zinc molybdate) with subsequent recrystallization in aqueous solutions (using zinc molybdate as a collector) was used. This technique was applied for the purification of the molybdenum sample which was used to synthesize the $ZnMoO_4$ compound. The first LU-MINEU crystals, consisting in several large $ZnMoO_4$ boules with high optical quality, were grown in platinum crucibles with $\oslash$ 40 and $\oslash$ 80 mm by using the LTG Cz technique and the produced $ZnMoO_4$ samples (with masses of 55 g and 160 g) were successfully tested above ground in a scintillating bolometer array [28].

Subsequently, a colorless large mass $ZnMoO_4$ crystal boule was grown in air atmosphere by directional solidification along the [001] crystalline axis. The boule was melted and then crystallized again. The growing conditions were as following: the temperature gradient did not exceed 1°C/cm, the rotational speed was set in the range of 5–20 rpm providing a crystallization rate around 1 mm per hour. The mass of the grown boule was at the level of 80% of the initial compound. The $ZnMoO_4$ boule and two produced large volume scintillation elements ($\oslash50\times40$ mm, masses of 336 and 334 g) are shown in Fig. 1 (b) and (d), respectively. The size of the scintillation elements are already compatible with the LUMINEU requirements and in general with a large-scale $0\nu2\beta$ decay experiment.

3. Tests of ZnMoO$_4$ radiopurity in the EDELWEISS set-up

3.1 Construction of ZnMoO$_4$-based scintillating bolometers

We used 313 g precursor (see Section 2.1) and 334 g advanced (see Section 2.2) ZnMoO$_4$ crystals to fabricate scintillating bolometers and to test their radiopurity. No special surface treatment was done except wiping with ultrapure ethanol. Each crystal, instrumented with two temperature sensors consisting of Neutron Transmutation Doped (NTD) Ge thermistors [31], was fixed inside an individual copper holder by using PTFE supporting elements. The NTD thermistors were glued by using six spots of $^{®}$Araldite epoxy glue and a 25 μm thick $^{®}$Mylar spacer, removed after the gluing operation. Two light detectors [32], consisting of $\varnothing$50×0.25 mm Ge disks and instrumented with NTD sensors, were mounted 2 mm above both plane faces of the precursor crystal to collect the emitted scintillation light. Only one Ge photodetector ($\varnothing$44×0.25 mm) was used for the bolometer based on the advanced ZnMoO$_4$ crystal. A reflector foil (VM2000/2002, 3M) was fixed inside the copper supports to improve light collection. A small heating element based on a heavily-doped silicon meander was glued by one epoxy spot on the surface of each ZnMoO$_4$ bolometer. This device has a steady resistance value and can be used to inject in the crystal stable-in-time amounts of thermal energy imitating the heat signals of the bolometer with the aim to control the stability of their thermal response [33]. NTD sensors and heating elements are read out through gold and aluminum wires respectively ($\varnothing$25 μm), ultrasonically bonded to metallic pads on a Kapton board glued on the copper holder. The NTD-sensor gold wires provide the thermal link of the detector to the heat sink.

3.2 Low background measurements in the EDELWEISS set-up

Both ZnMoO$_4$-based scintillating bolometers were tested in the EDELWEISS set-up [18], located deep underground ($\sim$4800 m w.e.) at the LSM (France). The laboratory location provides good background conditions, in particular the rock overburden suppresses the vertical muon flux to $\sim$ 5 μ/day/m^2 [34]; the total neutron flux is 9.6×10^{-6} n/day/cm^2 [35], which reduces to $\sim 1 \times 10^{-6}$ n/day/cm^2 above 1 MeV [36]. The EDELWEISS set-up is installed inside a clean room (ISO Class 4) and supplied by a deradonized ($\sim$30 mBq/m^3) air flow [37]. The EDELWEISS ^{3}He/^{4}He table-top dilution refrigerator with a large experimental volume (50 l) is surrounded by massive passive shields made of low radioactivity lead (20 cm minimum thickness) and polyethylene (50 cm minimum thickness). The set-up is completed by a muon veto (hermetic at $\sim$ 98.5% [34]), and by neutron and radon counters to control the external background. After the completion of the EDELWEISS-II experiment [18], the set-up was upgraded with improved thermal machines, ultra-radiopure internal copper screens and an inner polyethylene shielding.

The ZnMoO$_4$ precursor crystal was tested during the EDELWEISS-III commissioning run together with 15 FID (Fully InterDigit) bolometers based on ultra-pure Ge crystals (0.8 kg each) entirely covered with interleaved electrodes and dedicated to dark-matter search. After the conclusion of this run, the advanced ZnMoO$_4$ bolometer was installed with 36 FID detectors. The EDELWEISS-III physics run is in progress now in this configuration. The EDELWEISS set-up was further slightly upgraded between these two runs, but the only modification relevant to the ZnMoO$_4$ tests concerns the data acquisition system (DAQ). In the 15 FID run it was based on 14 bit ADC's for a part of the channels (including the readout of the precursor crystal) and 16 bit

ADC's for the rest; in the 36 FID run the 16 bit ADC's were extended to all the channels. In addition, the implementation of a correctly working pulser system, driving the stabilization heaters attached to each element of the scintillating bolometers, was completed during the data taking.

The data were recorded with 2 kHz and 1 kHz sampling rate for the precursor and the advanced $ZnMoO_4$ detectors respectively. The length of the pulse profile for the $ZnMoO_4$ bolometers was chosen around 2 s; half of this window contains information about baseline.

The base temperature during EDELWEISS-III commissioning run was stabilized at $\sim$ 19 mK, while it was decreased to $\sim$ 18 mK for the physics run. The resistances of the NTD sensors at such temperature conditions were around several MΩ. Difficulties encountered in the operation of the AC-bias electronics of EDELWEISS with working resistances in the 10-100 MΩ range prevented the taking of data at temperatures lower than $\sim$ 18 mK.

The background measurements with the precursor detector were conducted for a total 290 h live time duration. Two different gain settings both for the heat and the light channels were applied. Each setting was adopted for approximately half of the total acquisition time. Significantly higher statistics was accumulated over 2216 h with the bolometer based on the advanced $ZnMoO_4$ crystal. Only one gain setting was used for the heat channel, while several gain parameters were tested for the light channel of this detector. The data were processed off-line by using the optimum filter procedure [38] in order to extract the amplitude values related to each event both for the heat and the light signals and to maximize the signal-to-noise ratio.

The energy scale of the heat channels of the $ZnMoO_4$ bolometers was determined mainly with a ^{133}Ba γ reference calibration source, used in the standard EDELWEISS calibration procedure which is performed periodically. In addition, one calibration measurement for each detector was performed with a ^{232}Th source made of thoriated tungsten wires with a total mass of 15.2 g containing 1% of thorium in weight. The activity of this source ($\sim$ 600 Bq) was reduced by removing one half of the wires before the calibration of the advanced $ZnMoO_4$ detector. The Ba and Th sources were placed outside the cryostat during the calibrations. We removed a ^{55}Fe X-ray source,[2] normally used to irradiate permanently the rear side of our light detectors, in order to avoid any possible contamination of the inner volume of the cryostat.

The total energy spectra accumulated by the $ZnMoO_4$ scintillating bolometers in calibration measurements performed with the ^{133}Ba source are shown in Fig. 2. The energy resolution (FWHM) of the precursor detector at the 356 keV γ peak in the individual data sets was measured in the range of 6–13 keV giving a value of $\sim$ 7 keV FWHM for the total data set. The advanced $ZnMoO_4$ bolometer demonstrates excellent performance, in particular the energy resolution varied in the 3–5 keV range providing $\sim$ 4 keV FWHM for all the collected data. However, this better performance is not related to crystal quality, but to a more accurate choice of the detector operation point and DAQ parameters. The fluctuation of the filtered noise (baseline) was at the level of $\sim$ 1.5 keV FWHM for both detectors.

The performance of the $ZnMoO_4$ detectors in a wide energy interval (0.2–2.6 MeV) was tested in the calibration measurements with the ^{232}Th source, and the corresponding energy spectra are shown in Fig. 3. It is clear that the energy resolution of the 2614.5 keV γ peak of ^{208}Tl is worse than that for other peaks present in the spectra. In particular, the FWHM of this peak was measured

---

[2]This source is deposited on copper by drying a drop of ^{55}Fe-loaded acid .
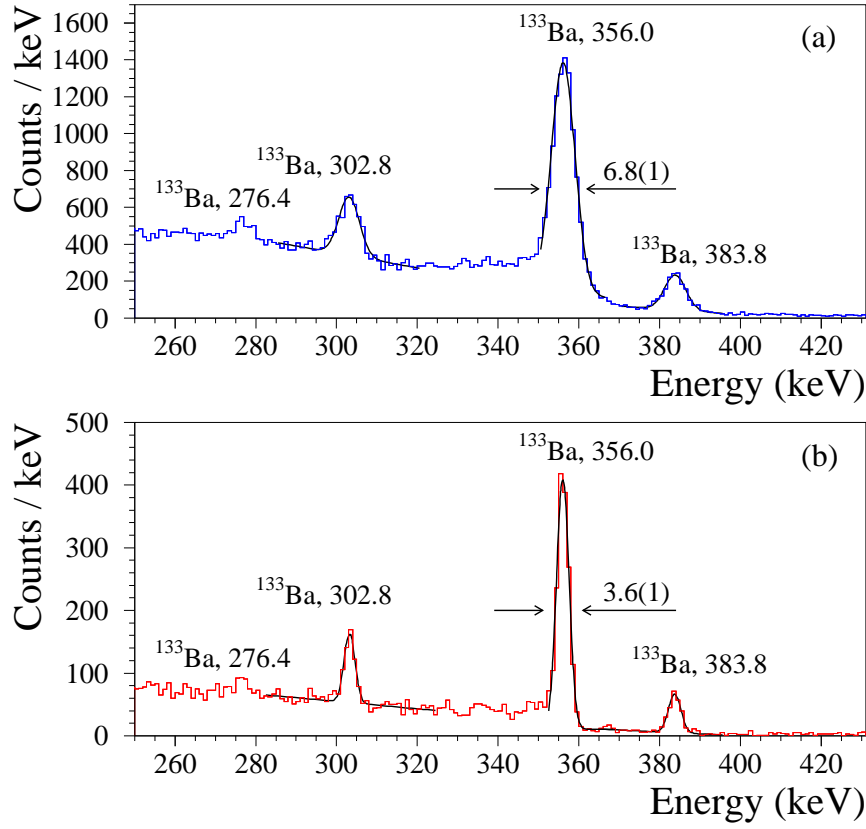
Figure 2. Energy spectra of the ^{133}Ba source measured by scintillating bolometers based on precursor (a) and advanced (b) ZnMoO$_4$ crystals in calibration runs collected over 513 h and 214 h of live time, respectively. The energy of gamma quanta and the resolution (FWHM) of the main ^{133}Ba line are given in keV. The fit of several γ peaks is also shown.

as 17(1) keV and 10(1) keV with the precursor and advanced ZnMoO$_4$ bolometers, respectively. During the same calibration, the FWHM value of the nearest intensive single peak, due to 911.0 keV γ's from ^{228}Ac, was 10(1) keV for the precursor and 5.0(4) keV for the advanced detector, respectively. These values are comparable to those obtained in the ^{133}Ba calibration. This poorer energy resolution at the 2614.5 keV γ line can be explained by pile-up effects due to the considerably high activity of the used ^{232}Th source. This is consistent with the results of the next data set for the precursor detector, in which the Th source was moved to another position in order to shield it by the FID Ge detectors. In these new conditions, a FWHM 9(2) keV energy resolution was measured at 2614.5 keV over 51 h of data taking. In these conditions, the data shown in Fig. 4 were collected, where the two-dimension distributions of the light and the heat signals measured in coincidence by the tested ZnMoO$_4$ scintillating bolometers are reported. Fig. 4 confirms the powerful particle identification capability of scintillating bolometers thanks to the different response of the ZnMoO$_4$ crystals to γ/β and α events.

3.3 Analysis of ZnMoO$_4$ radiopurity

The level of radiopurity of both tested ZnMoO$_4$ crystals was evaluated by using the data of the low
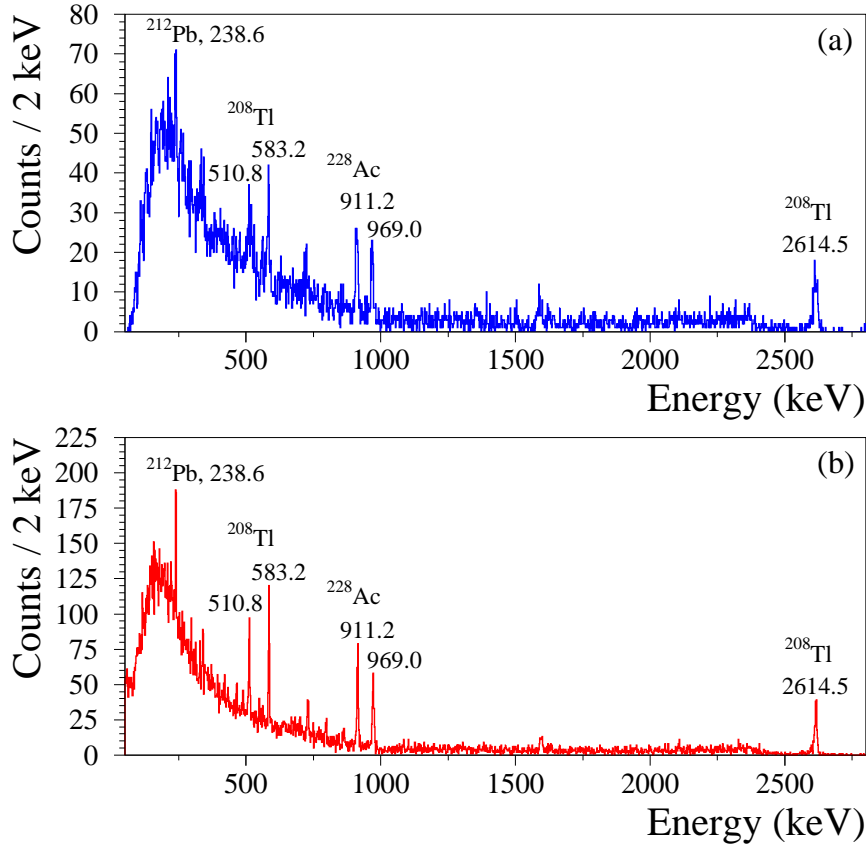
Figure 3. Energy spectra of a ^{232}Th source accumulated by scintillating bolometers constructed with precursor (a) and advanced (b) ZnMoO$_4$ crystals. The precursor was irradiated during 19 h, while the data from the advanced crystal were collected over 37 h. The energies of the most intensive γ peaks from the ^{232}Th chain are given in keV.

background measurements described above. Both the ^{133}Ba calibration and the background data were used for the precursor in order to have higher statistics and therefore to reach high enough sensitivity to the contaminants searched for. It is worth also noting that the EDELWEISS set-up has not been optimized yet for LUMINEU-like detectors, especially as far as the control of the vibration-induced noise is concerned. As a result, the light channel of the advanced ZnMoO$_4$-based bolometer was affected in several data sets by a severe microphonic noise which deteriorated the performance of the light detector. Therefore, in spite of excellent α/γ discrimination achieved with the ZnMoO$_4$ bolometers in selected runs, as demonstrated in Fig. 4, we did not apply this technique to discriminate different components of the background over the full data set. Taking into account that the dominant part of the γ/β background is located below 2.6 MeV, we used the data of the heat channels above 3 MeV for radiopurity analysis. In fact, this energy region is populated mainly by α's emitted by the radionuclides of the U/Th chains and therefore very sensitive to the internal radioactivity of the ZnMoO$_4$ crystals. Muon- and neutron-induced events give negligible contribution to the α background thanks to the underground conditions and the dedicated passive shields. Since the pulser system was operational only for a short fraction of the measurements with the advanced detector (the last 249 h), the stabilization of the thermal response
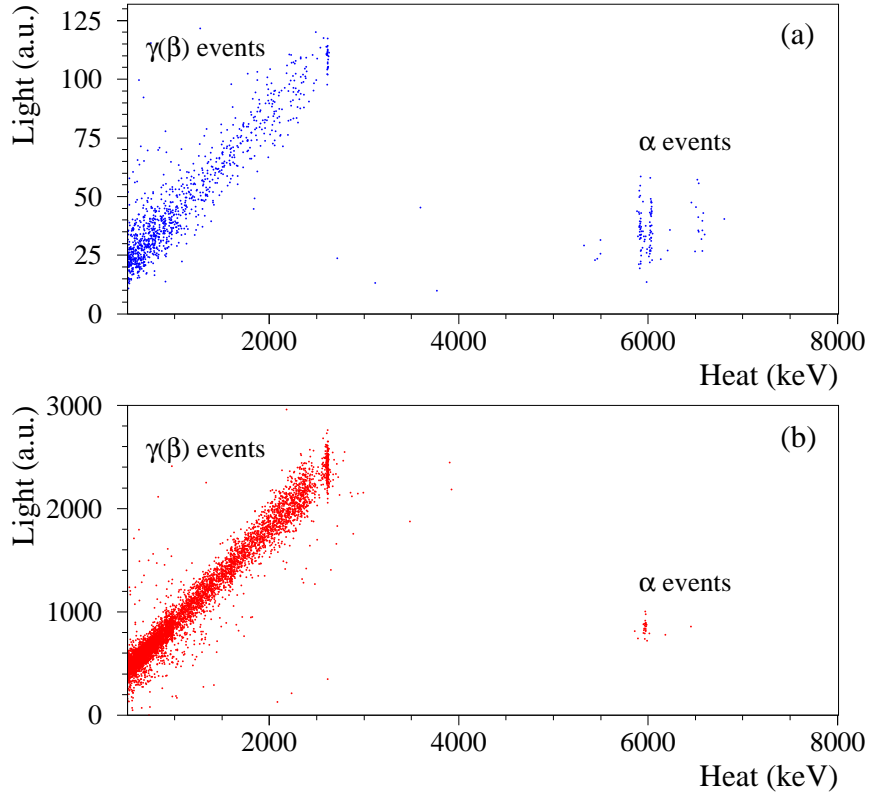
Figure 4. Scatter plots of light versus heat signals for the ZnMoO$_4$ scintillating bolometers accumulated in the calibration measurements with the ^{232}Th source. The data for the precursor crystal (a) were collected over 51 h (larger statistics than in Fig. 3); the advanced crystal (b) was irradiated during 37 h (same data as in Fig. 3). The α events (related with the internal contamination of the crystals and populated mainly by ^{210}Po – see text) are clearly separated from the γ/β band. The energy scale is determined by the γ calibration. The energy position of the α events is shifted by a factor $\sim$1.1 in this scale. This is due to a significantly different thermal response between α and γ/β events (details about quenching factors of heat signals are reported e.g. in Ref. [39]).

of the ZnMoO$_4$ detectors and the subsequent calibration of the α background was done by using the distribution of the α's emitted by the internal contamination of ^{210}Po. In the data fraction for which it was possible, we have compared heater-based stabilization with that obtained by using ^{210}Po signals, getting similar results.

The α spectra measured by both ZnMoO$_4$ bolometers – normalized on the live time of measurements and the mass of the crystals – are shown in Fig. 5. Several α peaks caused by trace internal radioactivity are visible. It is also evident from Fig. 5 that the advanced crystal has significantly higher purity with respect to the precursor. Below we consider in detail all the peculiarities observed in the spectra and their origin.

A clear pattern at 5.4 MeV in the data of both detectors visible in Fig. 5 is caused by the internal activity of ^{210}Po ($Q_\alpha = 5407.5$ keV, half-life = 138.376 d). (Here and later on Q's and half-lives are taken from Ref. [40] and [41].) First of all, we would like to note that it is rather difficult to derive from our data to what extent the equilibrium is broken in the ^{210}Pb-^{210}Po sub-chain, which
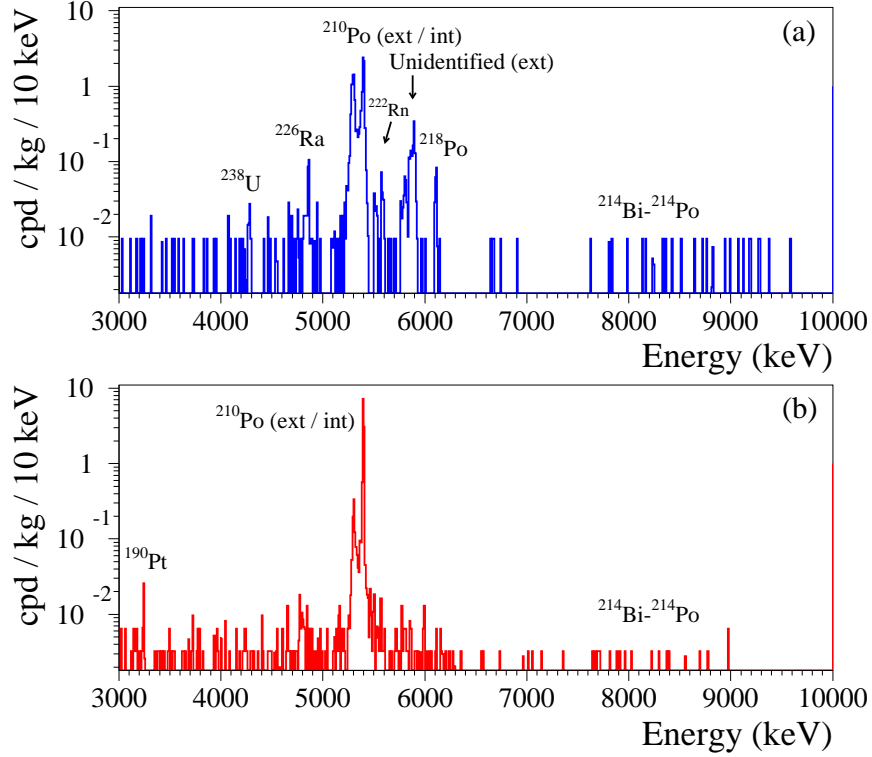
Figure 5. The α spectra collected in the low background measurements in the EDELWEISS set-up with scintillating bolometers based on the 313 g precursor (a) and the 334 g advanced (b) ZnMoO$_4$ samples operated over 803 h and 2216 h respectively. The origin of the α events providing the highest rates are indicated. The energy scale is determined by the α peaks. The labels "ext" and "int" refer to surface/external and bulk contamination, respectively.

is a section of the radon (^{222}Rn) progeny. There are however indications that the internal counts related to ^{210}Po are mainly due its progenitor ^{210}Pb (Q_β = 63.5 keV, half-life = 22.3 yr), since no appreciable decrease of the counts in the ^{210}Po internal activity of the advanced LUMINEU sample was observed over a period much longer (from August 2014 to March 2015) than the ^{210}Po half-life.

We would like to remark however that neither ^{210}Pb nor ^{210}Po are harmful for $0\nu2\beta$ decay search of ^{100}Mo, since they cannot populate the region of interest around 3034 keV, especially taking into account the excellent α/β rejection power of our technique. Therefore, we took for the moment no measure to reduce this contamination, which is by the way welcome at the present level of $\sim$ 1mBq/kg since it allows a continuous calibration of the α energy scale, offers a natural method to check and correct detector stability, and monitors the α/β rejection power in real time.

However, in the future we aim at controlling this contamination, which shows to be not very reproducible at this stage (it is present in both samples at the same order of magnitude, but it is definitely higher in the advanced crystal, as appreciable in Fig. 6 and in Table 1). It is well known that polonium and lead are highly volatile elements (see, e.g., Ref. [42]). We can preliminary assume therefore that they sublimated intensively together with molybdenum oxide during the sublimation step of the molybdenum purification procedure. Furthermore, some part of the ^{210}Po
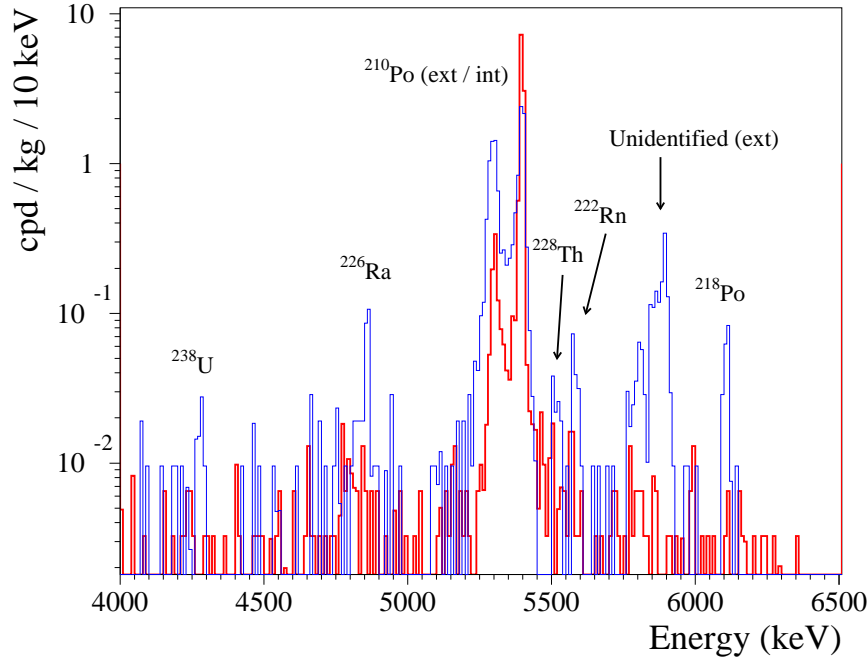
Figure 6. Zooms of the α spectra shown in Fig. 5 accumulated by the bolometers operated over 803 h with the precursor (blue line) and over 2216 h with the advanced (red line) ZnMoO$_4$ crystals. The shown energy interval corresponds to a range of Q_α values characteristic of most of the radionuclides of the U/Th chains.

contaminant could be explained by radon inclusion in the ZnMoO$_4$ compound and by accumulation of the long-living daughters ^{210}Pb and ^{210}Po due to ^{222}Rn short half-life ($\sim$ 3.8 d). In future crystal growth campaigns, we will revise our procedures assuming the correctness of these considerations.

Obviously, ^{210}Pb and ^{210}Po inclusion leads to a broken equilibrium in the ^{238}U chain, which is observed in the spectra. It is worth noting that broken equilibrium in the U/Th radioactive chains occurs in general in crystal scintillators, because some radionuclides can be separated during crystal production due to different chemical properties and this is the case for the tested ZnMoO$_4$ crystals. In addition to ^{210}Po, the data for the precursor crystal also exhibit a low α activity of ^{238}U and ^{226}Ra together with its daughters ^{222}Rn, ^{218}Po, and ^{214}Bi-^{214}Po events. In the case of the advanced crystal, a few counts are present in the ^{214}Bi-^{214}Po region but peak structures corresponding to ^{226}Ra and its daughters are not evident with the current statistics. Most of the peaks due to α decays in the U/Th chains are expected in the energy interval of 4–6.5 MeV which is shown in Fig. 6 for the α background of both ZnMoO$_4$ bolometers.

The data of the advanced crystal (see Fig. 5b) contain in the left part of the α spectrum a weak peak of ^{190}Pt ($Q_\alpha = 3252$ keV, 6.5×10^{11} yr), which is caused by a platinum contaminant due to ZnMoO$_4$ crystal growth in the platinum crucible. Such a contamination is also quite common for crystal scintillators and observed for example in TeO$_2$ crystals [43]. Only a hint on platinum contamination is visible for the precursor data, but the collected statistics was too low to observe this trace pollution with a high significance level.

A peak-like structure at 5.3 MeV corresponds to E_α of ^{210}Po ($E_\alpha = 5304.4$ keV) and indicates a surface contamination by ^{210}Po (or by its long-living progenitor ^{210}Pb) of the crystals and/or of

Table 1. Radioactive contamination of the advanced (LUMINEU) and precursor $ZnMoO_4$ crystals estimated from the α spectra accumulated in underground measurements at the LSM (France). The mass of the crystals and the total time of the accumulated data are also reported. The results for another large mass precursor, the 329 g $ZnMoO_4$ crystal which was operated as a scintillating bolometer during 524 h at the LNGS (Italy) [26], are given for comparison. The uncertainties are given at 68% C.L., while all the limits are calculated at 90% C.L. Note that column 2 reports the full released energies in α decays and not just the α energies.

Nuclide	Q_α-value [keV] [40]	Half-life [41]	Activity [μBq/kg]		
			LUMINEU crystal	Precursor crystals	
			334 g	313 g	329 g [26]
			2216 h	803 h	524 h
^{232}Th	4081.6 ± 1.4	1.405×10^{10} yr	≤ 2.3	≤ 5.5	≤ 8
^{228}Th	5520.08 ± 0.22	1.9116 yr	≤ 5.3	12 ± 4	≤ 6
^{238}U	4269.7 ± 2.9	4.468×10^9 yr	≤ 1.8	8 ± 3	≤ 6
^{234}U	4857.7 ± 0.7	2.455×10^5 yr	≤ 2.5	≤ 8.1	≤ 11
^{230}Th	4769.8 ± 1.5	7.538×10^4 yr	≤ 1.8	≤ 8.4	≤ 6
^{226}Ra	4870.62 ± 0.25	1600 yr	≤ 4.8	22 ± 5	27 ± 6
^{210}Po	5407.45 ± 0.07	138.376 d	1271 ± 22	703 ± 28	700 ± 30
^{235}U	4678.2 ± 0.7	7.038×10^8 yr	≤ 3.3	≤ 7.2	–
^{231}Pa	5150.0 ± 0.8	32760 yr	≤ 2.8	≤ 7.2	–
^{227}Th	6146.60 ± 0.10	18.72 d	≤ 2.8	≤ 3.8	–
^{223}Ra	5978.99 ± 0.21	11.435 d	≤ 3.8	≤ 5.5	–
^{190}Pt	3252 ± 6	6.5×10^{11} yr	3.8 ± 1.2	≤ 7.2	–
Unidentified (on surface)			–	134 ± 12	–

the construction components surrounding them. This effect is common in bolometers, which are detectors with no dead layer at the surface. It can be appreciated for example in TeO_2 bolometers (see e.g. Fig. 2 in Ref. [44] and, for an extensive discussion and detector response simulations, Ref. [45]). This surface contamination is much higher for the detector based on the precursor crystal, providing an α rate similar to that of the internal ^{210}Po. A bump at 5.75–5.9 MeV reveals another surface contaminant of the precursor detector but its origin has not been identified reliably.[3]

A possible explanation of this difference in surface contamination can be found in some aspects of the new protocol. The procedure to produce advanced $ZnMoO_4$ crystal scintillators was indeed improved in comparison to the precursor case: not only MoO_3 was deeply purified, but also synthesis of $ZnMoO_4$ powder was performed mainly in quartz and polypropylene lab-ware and surface polishing was done with the help of SiO_2 polishing powder, while rather contaminated car-

---

[3]This structure could be explained by the α-emitting radionuclide ^{244}Cm (Q_α = 5901.7 keV, half-life = 18.1 yr) which decays to long-live ^{240}Pu (Q_α = 5255.8 keV, half-life = 6563 yr). However, ^{244}Cm is not a naturally occurring radionuclide and, as it is synthesized in nuclear reactors, it is a quite rare metal. Therefore, the hypothesis of ^{244}Cm surface pollution should be taken with precaution.

borundum powder was utilised for the precursor surface treatment. At the same time, some steps of crystal production were made in the same conditions as of the precursor samples. Therefore, the reduction of ^{210}Po surface contamination will be especially addressed in the R&D which is in progress: we are going to use radiopure polishing materials and to minimize the time exposure to air of all the materials for crystal growth and production. We would like to stress anyway that one of the advantages of the scintillating bolometer technique is to make surface ^{210}Po α particles, which are often observed in bolometers, totally harmless for $0\nu2\beta$ decay search, as they can be efficiently tagged and no associated high-energy β particles are emitted.

Finally, a small excess of counts around 5.50–5.55 MeV (11 events) for the precursor data also indicates a possible contamination by ^{228}Th. The region of its daughter ^{224}Ra is affected by events from the unidentified surface contaminant and cannot be used to confirm this contamination. Other α emitting radionuclides in this sub-chain, ^{220}Rn and ^{216}Po, could appear in the data only as piled-up events due to the short half-life of ^{216}Po ($\sim$ 145 ms), which is comparable to the time response of the precursor-based detector (hundreds of ms). ^{212}Bi is not a sensitive way to confirm ^{228}Th contamination because in 64% of cases it gives unresolved β-α piled-up events from ^{212}Bi and ^{212}Po decays, populating the wide energy range 8.9–11.2 MeV, while only in the remaining 36% of cases it undergoes an α decay (Q_α = 6207.3 keV). Taking into account that there was no smooth data taking (we experienced several pauses related to cryogenic maintenance and daily 1 h regeneration of the FID detectors), α's from ^{212}Bi can be lost in the data due to the considerably long half-life of its mother nucleus ^{212}Pb (10.6 h). Therefore, the search for ^{220}Rn-^{216}Po overlapped events was performed and five observed α-pairs are in reasonable agreement with the ^{228}Th structure confirming this contamination.

Since there are no other α lines observed in the spectra, only limits can be set on activities of other radionuclides from U/Th families. The activities (or limits) of all α radionuclides searched for were obtained from the area of the peaks calculated over three σ intervals with the median at the expected Q_α values. The parameter σ was determined from the fit of the 5.4 MeV peak of internal ^{210}Po (FWHM = 18(1) and 9(1) keV for the precursor and the advanced crystals, respectively). Two energy regions (3.4–4 and 4.35–4.65 MeV) with a flat α continuum in which no peaks are expected were chosen to evaluate the background contribution. It was estimated as 0.96 and 1.25 counts per $\pm3\sigma$ interval for the precursor and the advanced crystals, respectively. The possible contribution of ^{226}Ra (Q_α = 4870.6 keV) to the area of ^{234}U (Q_α = 4857.7 keV) peak was subtracted. The number of counts excluded with 90% C.L. were calculated by using the Feldman-Cousins procedure [46].

All the derived activities (or limits) are summarized in Table 1 where the results of the recent measurements performed at the LNGS (Assergi, Italy) with a bolometer based on a similar size ZnMoO$_4$ crystal and produced from the same precursor boule are also given for comparison. The unprecedentedly high radiopurity of the LUMINEU crystal achieved thanks to the adopted purification and crystallization procedure is apparent. A significant progress is also reached in the reduction of the internal contamination of ^{226}Ra, which is not clearly detectable now while it was evident in both precursor crystals (313 and 329 g). The radiopurity levels of $\sim$0.005 mBq/kg achieved for ^{228}Th and ^{226}Ra (the most dangerous radionuclides for $0\nu2\beta$ searches) – even better than those considered in Ref. [3] ($\sim$0.01 mBq/kg) for very promising sensitivity evaluations of future ^{100}Mo searches – are therefore fully compatible with the purity requirements of next-generation $0\nu2\beta$ experiments capable to explore the inverted hierarchy region of the neutrino mass pattern [3, 4].

4. Conclusions

A significant progress in the development of large volume $ZnMoO_4$ crystal scintillators with excellent optical quality and high radiopurity has been achieved within the LUMINEU program. Two large volume crystal boules ($\sim$ 1 kg each) were grown by the low-thermal-gradient Czochralski technique. A slightly yellow colored boule, as a precursor of the LUMINEU project, was synthesized from high purity grade zinc and molybdenum oxides. A colorless crystal was developed within the LUMINEU program from molybdenum deeply purified by double recrystallization from aqueous solutions. Two $\sim$ 0.3 kg $ZnMoO_4$ samples were produced from each boule for low temperature tests.

Cryogenic tests of two scintillating bolometers based on the natural $ZnMoO_4$ crystals were performed in the EDELWEISS set-up at Modane Underground Laboratory (France). The detectors were operated over long term measurements and demonstrated high spectrometric performance and excellent α/γ discrimination. The measured radiopurity even of the precursor $ZnMoO_4$ crystal is very high. The observed trace internal contamination of this sample is related to ^{210}Po with activity at the level of 0.70(3) mBq/kg, ^{228}U (0.008(3) mBq/kg), ^{226}Ra (0.022(5) mBq/kg), and ^{228}Th (0.012(4) mBq/kg), while the activities of the other radionuclides from the U/Th chains and from ^{190}Pt are below 0.004–0.008 mBq/kg. Deep purification of molybdenum and recrystallization significantly improve the radiopurity of $ZnMoO_4$ crystals, in particular the activities of ^{228}Th and ^{226}Ra inside the LUMINEU crystal are below 0.005 mBq/kg. High collected statistics allows to observe a very weak activity of ^{190}Pt (0.004(1) mBq/kg) caused by a trace pollution by platinum due to crystal growth in a crucible made of this material. It is to note that the GDMS (Glow Discharge Mass Spectrometry) analysis of a crystalline sample from the LUMINEU boule has set a limit of 0.5 ppm on Pt contamination. In fact, the measured ^{190}Pt activity corresponds to 0.3(1) ppm, showing once again the superior sensitivity to trace contamination provided by direct internal α counting.

The extremely high radiopurity of $ZnMoO_4$ crystals, achieved within the LUMINEU program, totally satisfies the project requirements and opens the door to the application of $ZnMoO_4$-based scintillating bolometers to a next-generation $0\nu2\beta$ experiment aiming to investigate the inverted hierarchy region of the neutrino mass pattern.

Acknowledgments

References

[1] M. Tenconi et al. (for the LUMINEU collaboration), *LUMINEU: a pilot scintillating bolometer experiment for neutrinoless double beta decay search*, Physics Procedia **61** (2015) 782.

[2] S. Pirro et al., *Scintillating double-beta-decay bolometers*, Phys. Atom. Nucl. **69** (2006) 2109.

[3] J.W. Beeman et al., *A next-generation neutrinoless double beta decay experiment based on ZnMoO$_4$ scintillating bolometers*, Phys. Lett. **B710** (2012) 318.

[4] D.R. Artusa et al., *Exploring the neutrinoless double beta decay in the inverted neutrino hierarchy with bolometric detectors*, Eur. Phys. J. **C74** (2014) 3096.

[5] W. Rodejohann, *Neutrino-less Double Beta Decay and Particle Physics*, Int. J. Mod. Phys. **E20** (2011) 1833.

[6] S.R. Elliott, *Recent progress in double beta decay*, Mod. Phys. Lett. **A27** (2012) 1230009.

[7] J.D. Vergados, H. Ejiri, F. Simkovic, *Theory of neutrinoless double-beta decay*, Rep. Prog. Phys. **75** (2012) 106301.

[8] A.S. Barabash et al., *Enriched Zn^{100}MoO$_4$ scintillating bolometers to search for $0\nu2\beta$ decay of ^{100}Mo with the LUMINEU experiment*, Eur. Phys. J. **C74** (2014) 3133.

[9] L.G. Van Uitert, J.J. Rubin, W.A. Bonner, *Preparation of Single Crystals of Tungstates and Molybdates of a Number of Divalent Metal Ions*, J. American Ceramic Soc. **46** (1963) 512.

[10] S.C. Abrahams, *Crystal Structure of the Transition-Metal Molybdates and Tungstates. III. Diamagnetic α-ZnMoO$_4$*, J. Chem. Phys. **46** (1967) 2052.

[11] V.B. Mikhailik et al., *Optical and luminescence studies of ZnMoO$_4$ using vacuum ultraviolet synchrotron radiation*, Nucl. Instr. Meth. **A562** (2006) 513.

[12] L.I. Ivleva et al., *Growth and Properties of ZnMoO$_4$ Single Crystals*, Crystallography Rep. **53** (2008) 1087.

[13] L.L. Nagornaya et al., *Tungstate and Molybdate Scintillators to Search for Dark Matter and Double Beta Decay*, IEEE Trans. Nucl Sci. **56** (2009) 2513.

[14] L. Gironi et al., *Performance of ZnMoO$_4$ crystal as cryogenic scintillating bolometer to search for double beta decay of molybdenum*, JINST **5** (2010) P11007.

[15] A.M. Dubovik et al., *Research and Development of ZnBO$_4$ (B = W, Mo) Crystal Scintillators for Dark Matter and Double Beta Decay Searching*, Acta Phys. Pol. **A117** (2010) 15.

[16] A.A. Pavlyuk et al., *Low Thermal Gradient technique and method for large oxide crystals growth from melt and flux*, in *Proc. of the APSAM-92*, Asia Pacific Society for Advanced Materials, Shanghai, 26–29 April 1992, Institute of Materials Research, Tohoku University, Sendai, Japan, 1993, p. 164.

[17] Ya.V. Vasiliev et al., *BGO crystals grown by a low thermal gradient Czochralski technique*, Nucl. Instr. Meth. **A379** (1996) 533.

[18] E. Armengaud et al., *Final results of the EDELWEISS-II WIMP search using a 4-kg array of cryogenic germanium detectors with interleaved electrodes*, Phys. Lett. **B702** (2011) 329.

[19] A. Borovlev et al., *Progress in growth of large sized BGO crystals by the low-thermal-gradient Czochralski technique*, J. Cryst. Growth **229** (2001) 305.

[20] E.N. Galashov, V.A. Gusev, V.N. Shlegel, Ya.V. Vasiliev, *The growth of ZnWO$_4$ and CdWO$_4$ single crystals from melt by the low thermal gradient Czochralski technique*, Crystallogr. Rep. **54** (2009) 689.

[21] P. Belli et al., *Development of enriched ^{106}CdWO$_4$ crystal scintillators to search for double β decay processes in ^{106}Cd*, Nucl. Instrum. Meth. **A615** (2010) 301.

[22] A.S. Barabash et al., *Low background detector with enriched* $^{116}CdWO_4$ *crystal scintillators to search for double β decay of* ^{116}Cd, *JINST* **6** (2011) P08011.

[23] http://www.zincchemicals.umicore.com/ZincChemicals/

[24] P. Belli et al., *Radioactive contamination of* $ZnWO_4$ *crystal scintillators*, *Nucl. Instrum. Meth.* **A626-627** (2011) 31.

[25] E.N. Galashov, P.S. Galkin, P.E. Plusnin, V.N. Shlegel, *Specific features of the phase formation, synthesis, and growth of* $ZnMoO_4$ *crystals*, *Crystallogr. Rep.* **59** (2014) 288.

[26] J.W. Beeman et al., *Performances of a large mass* $ZnMoO_4$ *scintillating bolometer for a next generation 0νDBD experiment*, *Eur. Phys. J.* **C72** (2012) 2142.

[27] D.M. Chernyak et al., *Optical, luminescence and thermal properties of radiopure* $ZnMoO_4$ *crystals used in scintillating bolometers for double beta decay search*, *Nucl. Instr. Meth.* **A729** (2013) 856.

[28] L. Bergé et al., *Purification of molybdenum, growth and characterization of medium volume* $ZnMoO_4$ *crystals for the LUMINEU program*, *JINST* **9** (2014) P06004.

[29] J.W. Beeman et al., *An Improved* $ZnMoO_4$ *Scintillating Bolometer for the Search for Neutrinoless Double Beta Decay of* ^{100}Mo, *J. Low Temp. Phys.* **167** (2012) 1021.

[30] J.W. Beeman et al., $ZnMoO_4$: *A promising bolometer for neutrinoless double beta decay searches*, *Astropart. Phys.* **35** (2012) 813.

[31] E. Haller, *Isotopically engineered semiconductors*, *J. Appl. Phys.* **77** (1995) 2857.

[32] M. Tenconi et al., *Bolometric light detectors for neutrinoless double beta decay search*, PoS (PhotoDet 2012) 072.

[33] A. Alessandrello et al., *Methods for response stabilization in bolometers for rare decays*, *Nucl. Instrum. Meth.* **A412** (1998) 454.

[34] B. Schmidt et al., *Muon-induced background in the EDELWEISS dark matter search*, *Astropart. Phys.* **44** (2013) 28.

[35] K. Eitel et al., *Measurements of neutron fluxes in the LSM underground laboratory*, *J. Phys.: Conf. Ser.* **375** (2012) 012016.

[36] S. Fiorucci et al., *Identification of backgrounds in the EDELWEISS-I dark matter search experiment*, *Astropart. Phys.* **28** (2007) 143.

[37] E. Armengaud et al., *Background studies for the EDELWEISS dark matter experiment*, *Astropart. Phys.* **47** (2013) 1.

[38] E. Gatti, P. Manfredi, *Processing the signals from solid-state detectors in elementary-particle physics*, *Riv. Nuovo Cim.* **9** (1986) 1.

[39] C. Arnaboldi et al., $CdWO_4$ *scintillating bolometer for Double Beta Decay: Light and heat anticorrelation, light yield and quenching factors*, *Astropart. Phys.* **34** (2010) 143.

[40] M. Wang et al., *The AME2012 atomic mass evaluation * (II). Tables, graphs and references*, *Chinese Phys.* **C36** (2012) 1603.

[41] R.B. Firestone et al., *Table of Isotopes*, 8-th ed., John Wiley, New York, 1996 and CD update, 1998.

[42] S.K. Sahu et al., *Enrichment and particle size dependence of polonium and other naturally occurring radionuclides in coal ash*, *J. Environ. Radioact.* **138** (2014) 421.

[43] F. Alessandria et al., *CUORE crystal validation runs: results on radioactive contamination and extrapolation to the CUORE background*, Astropart. Phys. **35** (2012) 839.

[44] D.R. Artusa et al., *Searching for Neutrinoless Double-Beta Decay of ^{130}Te with CUORE*, Adv. High En. Phys. **2015** (2015) 879871.

[45] L. Pattavina, PhD thesis, *Radon-induced surface contaminations in neutrinoless double beta decay and dark matter experiments*, Università degli Studi di Milano-Bicocca and Université Claude Bernard Lyon 1, 2011.

[46] G.J. Feldman, R.D. Cousins, *Unified approach to the classical statistical analysis of small signals*, Phys. Rev. **D57** (1998) 3873.